

One-dimensional character of miniband transport in doped GaAs/AlAs superlattices

Yu. A. Pusep, A. J. Chiquito, S. Mergulhão, and J. C. Galzerani

Departamento de Física, Universidade Federal de São Carlos, Caixa Postal 676, 13565-905 São Carlos, São Paulo, Brazil

(Received 11 March 1997)

Evidence of the crucial role of random fluctuations of the well size in vertical transport in doped GaAs/AlAs superlattices with broad minibands has been obtained by both Fourier-transform reflection spectroscopy and C - V measurements. It turned out that even monolayer fluctuations of the periodicity, or random fluctuations of the impurity potentials, which are unavoidable, can cause a partial localization of electrons providing one-dimensional conducting channels where the periodicity is conserved, and through which the electron transport across the superlattice would occur. This was found to be the reason why, instead of the constant vertical conductivity (independent of the electron density) predicted by the theory to occur when the Fermi energy exceeds the miniband width, a drop of the conductivity giving a metal-to-dielectric phase transition was observed. [S0163-1829(97)01731-1]

I. INTRODUCTION

Since the first proposal of semiconductor superlattices (SL's) consisting of periodic alteration of two compounds,¹ they have been extensively studied from different points of view. Transport properties of electrons in SL's attracted much attention because of the predicted negative differential conductance (NDC) (Ref. 1) and Bloch oscillations;² both have been shown to occur due to the miniband character of the electron transport, or, more explicitly, due to the finite miniband width. However, in the earliest presentation of NDC,³ it was established that it is not the miniband effects but the high-electric-field domains arising due to fluctuations of the electron potential of a SL that are responsible for the observed effect. This showed the importance of the electron potential fluctuations influencing the character of the vertical (perpendicular to the layers) transport in a SL. Later, the electric-field-induced localization of the electron wave functions (the Wannier-Stark effect) has been found to be an additional reason for NDC.^{4,5} Both observations presented the influence of the external electric field on the character of vertical transport, when the electric field applied to a sample in order to measure the conductivity is strong enough to disturb significantly the periodic potential of a SL breaking down the minibands.

When optical measurements are applied, the external electric field (which is the electric field of light) is too small to disturb the electron miniband structure. Therefore, spectroscopical methods (for instance, measurement of an electron plasma resonance) give us the conductivity at an optical frequency, and allow us to study the electron transport in an original, not disturbed, SL potential. Moreover, optical spectroscopy makes it possible to separate the energy and the relaxation time of electron plasma excitations which contribute as the product to a conductivity. This additional advantage turns out to be important in assigning an origin to electron transport in SL's.

To our knowledge, the first application of optical spectroscopy to a study of the problems related to vertical transport and electron localization in artificially disordered SL's was presented in Ref. 6, where the photoluminescence (PL)

was used to detect electrons passing through a SL. However, PL measurements do not allow a quantitative analysis of the electron transport, because the PL amplitude giving the electron transport intensity also depends strongly on the electron transition probability which is not known for certain.

In our recent papers,^{7,8} we proposed Fourier-transform infrared (FTIR) spectroscopy as a tool to probe the vertical conductivity in semiconductor SL's by means of the measurement of the plasma frequency of free electrons in a partly occupied miniband. In addition to the above-mentioned advantages of optic methods, FTIR makes a quantitative analysis possible, and, when p -polarized reflection (or absorption) spectra are taken, FTIR selects only the plasma modes polarized normal to the layers and, thus, probes only the movement of electrons along the periodic potential (vertical transport).^{7,8}

By means of FTIR spectroscopy, one can measure the vertical conductivity

$$\sigma_z(\omega) = \frac{\sigma_z(0)}{1 + \omega^2 \tau_{pz}^2}, \quad (1)$$

with $\sigma_z(0) = \omega_{pz}^2 \tau_{pz} / \pi$, where $\omega_{pz}^2 = 4\pi e^2 n / m_z$ is the frequency of the plasma vibrations polarized along the growth direction of a SL (the z direction) with the electron density n and the electron effective mass in the z direction m_z , and τ_{pz} is the relaxation time of plasmons. In order to study the miniband dispersion, the plasma frequency ω_{pz} can be measured in SL's, with the electron densities varying with the doping level. The variation of the electron density changes the vertical conductivity in a significantly different way when compared with the variation caused by an applied electric field. As was already pointed out, the rise of an applied bias to a SL produces the NDC due to the miniband effects—electrons accelerated until the top of the miniband became heavier, thus decreasing the current through the SL. Similarly, it seems that the conductivity should decrease because of the increase of the electron effective mass when the Fermi energy (E_F) reaches the top of the miniband. However, as was first established in Ref. 9, the vertical conductivity does not decrease even when the Fermi energy reaches the top of

a miniband; rather, it reveals a steplike dependence on the Fermi energy, when a plateau with a nonzero conductivity occurs at the Fermi level located in a minigap between two minibands. This is because of the unique form of the Fermi surface in a SL. That is, when the Fermi level enters a minigap, both the Fermi velocity (v_F) and the two-dimensional (2D) density of electron states (N_{2D}), which contribute to the vertical conductivity, remain constant until E_F enters the next miniband.

When $\hbar/\tau_{pz} < E_F$ the steplike dependence of the vertical conductivity on the Fermi energy has been found to obey the formula:⁹

$$\sigma_z(E_F) = \frac{n^* e^2 \tau_{pz}(E_F)}{m_z}, \quad (2)$$

with

$$n^* = \frac{m_x W}{2\hbar^2 d_{SL} \pi^2} (k_F d_{SL} - 0.5 \sin 2k_F d_{SL}), \quad (3)$$

$$k_F = \begin{cases} 0, & E_F < 0 \\ d_{SL}^{-1} \cos^{-1} \left(\frac{W - E_F}{W} \right), & 0 < E_F < 2W \\ \pi/d_{SL}, & E_F > 2W, \end{cases} \quad (4)$$

where m_x is the electron effective mass parallel to the layers, W is the miniband half-width, and d_{SL} is the SL period, respectively.

In contrast, a consideration of the one-dimensional periodic potential shows a zero conductivity when the Fermi energy is inside a minigap. In such a manner, the 1D transport in a SL reveals a metal-dielectric phase transition when the Fermi energy exceeds the miniband width, while such a transition does not occur when the three-dimensional electron states contribute. This shows the importance of the full 3D consideration of the vertical transport problem in SL's.

The problem related to this paper can be formulated as follows—does the vertical transport in SL's indeed have 3D character? To resolve this problem we studied vertical transport in doped GaAs/AlAs SL's by FTIR reflection spectroscopy and by C - V measurements.

It was found that because of the fluctuations of the periodic potential of a SL at high enough doping densities, the electron transport is limited in space—electrons move in the 1D conductive channels where the nominal periodicity is conserved. This 1D character of the electron transport results in a metal-dielectric phase transition shown to occur with the increase of the electron density, in accordance with the prediction of the 1D model. The C - V measurements confirmed the existence of localized electron states in the SL's under investigation.

II. EXPERIMENT

The samples used in this study were grown by molecular-beam epitaxy on (100) GaAs substrates, and were composed of GaAs/AlAs Si-doped SL's with 17 or 25 ML of GaAs quantum wells and extremely thin (2 ML thick) AlAs barriers; the period was repeated 40 times in each sample. A 1- μm -thick n^+ GaAs:Si buffer layer was grown between the

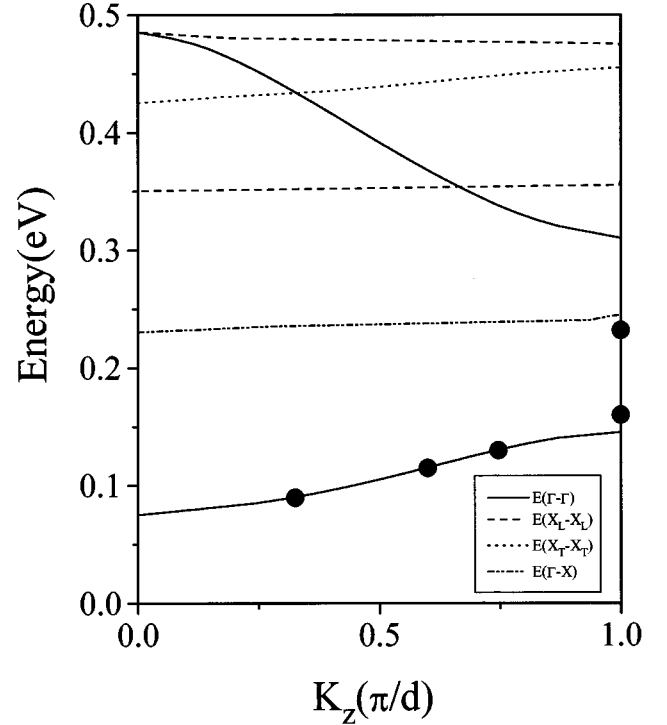


FIG. 1. The electron energy structure of the $(\text{GaAs})_{17}(\text{AlAs})_2$ superlattice. The full circles show the positions of the Fermi energies in the differently doped samples under investigation: 1×10^{17} , 7×10^{17} , 1.4×10^{17} , 2.8×10^{17} , and $5.6 \times 10^{17} \text{ cm}^{-3}$. The inset shows the types of the electron states of GaAs wells and AlAs barriers considered in the calculations.

substrate and the SL in order to increase the reflectivity, and to allow the fabrication of a contact to the backside of the SL's.

For the C - V measurements the Ohmic contact to the substrate was made by evaporation of a Au-Ge-Ni alloy followed by an annealing at 450 °C, while an Al contact evaporated on the surface of the SL was utilized as a Schottky contact. The densities of electrons in the samples were taken as the nominal doping densities. For the low-doped samples the values of the electron concentration were obtained by the C - V measurements as well.

The electron energy structure of the $(\text{GaAs})_{17}(\text{AlAs})_2$ SL's calculated in the envelope-function approximation is displayed in Fig. 1. The full circles show the positions of the Fermi energy for the samples with the electron densities $n_e = 1 \times 10^{17}$, 7×10^{17} , 1.4×10^{17} , 2.8×10^{17} , and $5.6 \times 10^{17} \text{ cm}^{-3}$. All the parameters indispensable to the calculations were taken from Ref. 10. The calculations show that the lowest broad Γ miniband with a width of 70 meV is separated from the high-lying Γ miniband by an energy of approximately 160 meV. The doping was made in order to vary the positions of the Fermi level in different samples from the bottom of the Γ miniband until the minigap, crossing the top of the miniband.

The p -polarized reflection spectra were taken at $T = 80 \text{ K}$ with a Bruker IFS - 113-V Fourier-transform infrared spectrometer. The C - V data were measured at $T = 8 \text{ K}$. The details of the spectroscopic analysis can be found in Ref. 8.

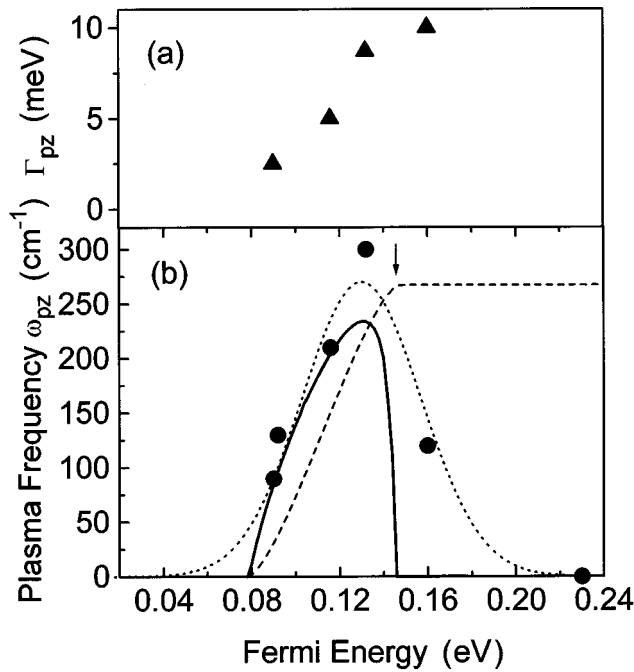


FIG. 2. The dependence of the plasma frequency ω_{pz} on the Fermi energy measured in the $(\text{GaAs})_{17}(\text{AlAs})_2$ superlattices with different doping (a). The results of the 3D calculations obtained by formula (2) are shown by the dashed line. The full line represents the data obtained by the 1D envelope-function approximation calculations. The dotted line shows the energy distribution of the localized states in the first Γ miniband as it was used in the calculations of the temperature dependence of a capacitance. The top panel (b) displays the values of $\Gamma_{pz} = \hbar/\tau_{pz}$ as obtained by the fitting of the reflection spectra.

III. RESULTS AND DISCUSSION

The values of the plasma frequencies ω_{pz} associated with the collective vibrations of electrons parallel to the superlattice axis (z direction) obtained by the reflection spectra in Ref. 8 are collected in Fig. 2 for the samples with different doping levels. Dependencies calculated by means of the modeling of the 1D transport when a one-dimensional periodic potential was taken into account, and by the theory of the 3D conductivity,⁹ are presented in Fig. 2 as well. The 3D calculations are fulfilled according to the formulas (2)–(4). As was seen, our experimental results show a 1D behavior rather than a 3D one, and reveal a metal-dielectric transition at the Fermi energy corresponding to the top of the lowest Γ miniband [shown by the arrow in Fig. 2(b)]. It should be mentioned that no fitting parameters were used in these calculations. Thus it seems that the 2D electron states taken into account in the full 3D consideration⁹ do not contribute to the vertical conductivity.

This surprising result can be understood if we take the fluctuations of periodicity into consideration. Such fluctuations can result from random layer-thickness fluctuations which have very different lateral extinction (L_0) varying from some tens of angstroms¹¹ to a few micrometers.¹² The calculations show that in our samples even the unavoidable monolayer layer-thickness fluctuations give the average electron energy fluctuations $\hbar/\tau_{MD} \approx 80\text{--}90$ meV, which exceed the width of the lowest Γ miniband ($\Delta_1 \approx 70$ meV). This estimation gives the minimum value of the electron energy

fluctuations; actually, the layer-thickness fluctuations can exceed the monolayer width. Moreover, the random potential of impurities can influence the SL potential and cause additional electron localization. These effects will disturb the coherence between electron wave functions in neighbor quantum wells enough to cause disordered spatial localization. The correlation length of fluctuations of periodicity can be long enough to form conducting channels; some of them can overlap, providing the vertical transport through the SL with a percolative character.

Apparently, such a vertical transport will have 1D character when the lateral width of the conducting channels is smaller than the wavelength of the electrons (λ_e). The minimum wavelength of the electrons in a SL miniband is $2d_{\text{SL}}$. For the samples studied here, this means $\lambda_e \approx 200$ Å. Thus the condition for one-dimensional transport through the conducting channels will be fulfilled for $L_0 \leq 200$ Å. If impurities are responsible for the violation of the periodicity of a SL, then the doping density of $8 \times 10^{18} \text{ cm}^{-3}$ will give such a value of L_0 .

In order to confirm the effect of the spatial electron localization and thus, the existence of the 1D conducting channels in the SL's under investigation, we measured the capacitance of the Schottky junction fabricated on the surface of the samples. This is considered one of the primary methods for studying the trapping by deep-level defects or impurities.¹³

To find evidence of trapping due to the localized electron levels, we examined the temperature dependence of the capacitance in a temperature range from 8 to 300 K. In this temperature range the band-to-band electron activation in the GaAs/AlAs SL's is negligible, and, thus, we would expect that in the presence of localized electron states we would be able to observe an alteration of the capacitance due to their thermal activation.

Figure 3 presents results obtained on some of the studied samples (the capacitance of the SL's with doping levels larger than 10^{18} cm^{-3} could not be measured because of the influence of the built-in electric field at the surface of the sample). These results show the increase of the capacitance with temperature. The value of the capacitance can be obtained from

$$C = \frac{4\pi S}{W}, \quad (5)$$

where S is the measured area and W is the width of the depletion layer. In the SL's under investigation, $W = (6\pi n e^2 / E_F)^{-1/2} \sim n^{-1/6}$ because of the Thomas-Fermi screening. The increase of the free-electron density estimated by means of the measured $C(T)$ dependencies reveals an activation energy about 200 meV, which is comparable to the width of the lowest first Γ miniband, and to the energy gap between the first and the second Γ minibands. Therefore, it is clear that at least part of the electron states of the first Γ miniband should be localized, and the thermalization of the electrons from the first miniband to the second one should be considered to supply the observed increase of the capacitance.

In order to analyze the temperature dependence of the capacitance measured in the SL's, we treated the simple model with two minibands: in the lowest miniband the elec-

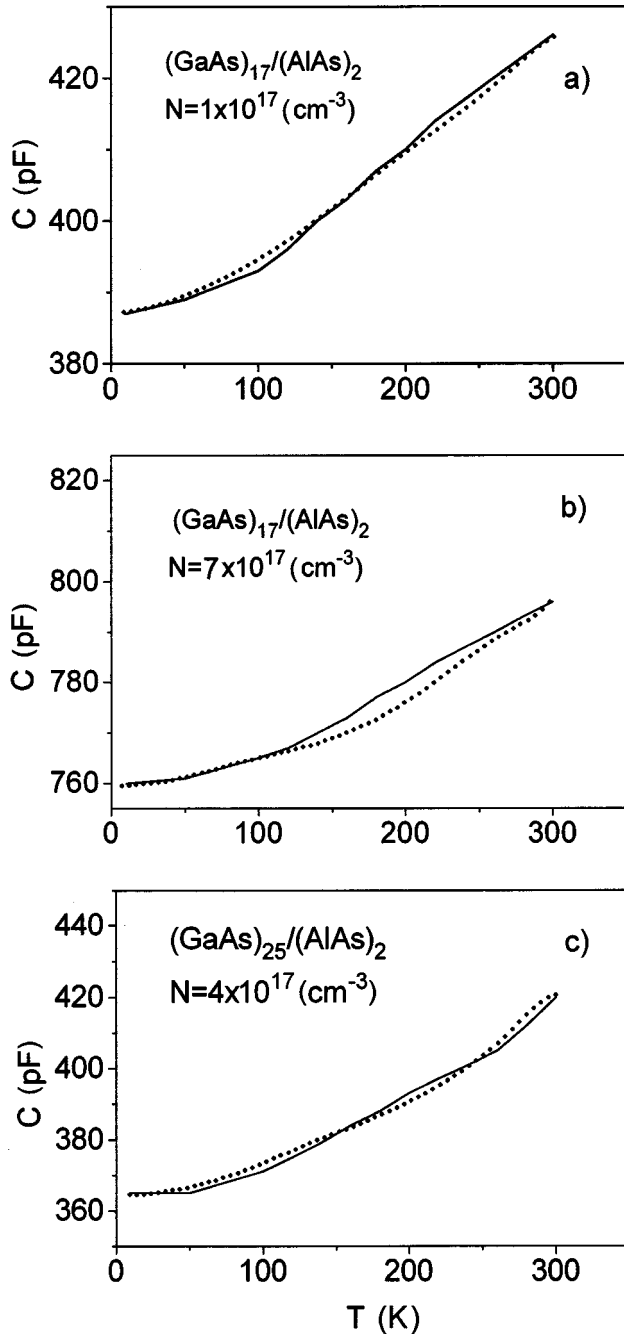


FIG. 3. The dependence of a capacitance on temperature for the Schottky devices made of the doped superlattices $(\text{GaAs})_{17}/(\text{AlAs})_2$ with $n = 1 \times 10^{17} \text{ cm}^{-3}$ (a), $7 \times 10^{17} \text{ cm}^{-3}$ (b), and $(\text{GaAs})_{25}/(\text{AlAs})_2$ with $n = 4 \times 10^{17} \text{ cm}^{-3}$ (a). The full lines were computed by the two-miniband model described in the text with the percentage of the localized electron states in the lowest miniband: (a) –4%, (b) –30%, and (c) –60%.

trons can be fully localized, while all the electrons in the high-lying miniband are delocalized.

In spite of its simplicity, this model seems to be quite realistic because, as was mentioned above, even the monolayer width fluctuations can cause a breakdown of the coherency between electron states in the lowest Γ miniband, while they can cause only partial electron localization in the second one. Moreover, the estimation of the activation energy from the $C(T)$ dependencies gives a value which exceeds the

width of the first Γ miniband; this also implies that most of the electron states belonging to this miniband should be localized. Thus in our model the thermal excitation of electrons from the localized states of the first Γ miniband to the second one produces the free electrons which contribute to the rise of the capacitance.

In order to calculate the concentration of the thermalized electrons, we numerically solved the equation

$$\int_{\Delta_1} \frac{N_1(E)dE}{1 + \frac{1}{2} \exp \frac{E-\mu}{kT}} + \int_{\Delta_2} \frac{N_2(E)dE}{1 + \exp \frac{E-\mu}{kT}} - n_e = 0, \quad (6)$$

where the chemical potential μ is unknown, n_e is the total electron density, and $N_1(E)$ and $N_2(E)$ are the densities of electrons states in the first and second Γ minibands, respectively. The chemical potential found as a solution of this equation was substituted into the second term of Eq. (6) to obtain the electron concentration in the second miniband (n_2).

We approximated $N_1(E)$ by the Gauss distribution function, with a full width at half maximum equal to the width of the first miniband calculated by the envelope-function approximation (EFA). The density of localized states was normalized with respect to the density of states in an unperturbed miniband (calculated by the EFA). The energy distribution of the localized electron states in the first miniband obtained in such a manner is depicted in Fig. 2. $N_2(E)$ was calculated by the EFA. Finally, the capacitance of the SL was computed from relation (5) with $n = n_2$, and then normalized with respect to the measured values.

However, this model gives dependencies of $C(T)$ stronger than were observed in experiment. Thus, if all the electron states in the lowest miniband are localized, the calculated increase of the capacitance with temperature is too large; if, on the contrary, all the electrons are delocalized, no rise of capacitance occurs. Therefore, this means that electron states in the lowest miniband are partly localized. These delocalized electron states belong to the conducting channels and contribute to the conductivity, but do not contribute to the capacitance; the localized ones contribute to the capacitance and not to the conductivity. The best fitting of the computed $C(T)$ dependencies to the experimental ones (results are shown in Fig. 3) was obtained with the percentage of the localized electron states given in Fig. 3.

It turned out that a few electron states are localized in the $(\text{GaAs})_{17}/(\text{AlAs})_2$ SL with an electron concentration 10^{17} cm^{-3} ; however, their number significantly increases with an increase of the doping level, which reflects the strong influence of impurities on the electron localization. The increase of the number of localized electron states observed with the increase of the doping allows us to conclude that more than half of all the electron states of the lowest Γ miniband are localized in a SL with a doping density larger than $2 \times 10^{18} \text{ cm}^{-3}$, where the formation of the 1D conducting channels was detected.

It is clear that, the narrower the miniband, the stronger the localization that will be caused by the same doping density. This was indeed observed in the $(\text{GaAs})_{25}/(\text{AlAs})_2$ SL where the width of the first Γ miniband equals 32 meV; here more than half of the electrons become localized at a doping den-

sity of $4 \times 10^{17} \text{ cm}^{-3}$ (the position of the Fermi level in this sample was found to be close to the top of the first Γ miniband).

It is worth mentioning that the full localization of the electron states in the lowest miniband which may occur in SL's with extremely high doping densities will cause a quantum-mechanical broadening of the vertical plasmon $\Gamma_{pz} = \hbar/\tau_{pz}$ exceeding the width of the miniband, which was not observed experimentally. Conversely, as depicted in Fig. 2(a), the values of Γ_{pz} found by the fitting the reflection spectra are much smaller than the width of the miniband even in the highly doped samples. Therefore, we conclude that these values of Γ_{pz} instead relate to plasma vibrations in the conducting channels.

It should be mentioned that in our simple model we did not include the partial localization which can occur in the second Γ miniband. It is clear that this will cause an increase of the effective gap between the minibands and, consequently, a decrease of the number of localized states obtained by the fitting. This effect is expected to be stronger in SL's with narrower minibands. Therefore, although a quantitative analysis could not yet be performed, the model utilized gives a quite correct qualitative explanation of the obtained results.

IV. CONCLUSIONS

We have investigated the vertical transport in doped GaAs/AlAs SL's with broad minibands by FTIR reflection spectroscopy. No external electric field which could disturb the SL periodic potential was applied to the samples. Instead

of the expected plateaulike behavior of the vertical conductivity predicted by the theory⁹ to occur when the Fermi level enters a minigap between two minibands, a metal-to-dielectric transition was found, which is the characteristic feature of the 1D transport. This result can be explained if random fluctuations of the superlattice periodicity are taken into consideration. Such fluctuations can cause the spatial localization of electrons providing 1D conducting channels to transfer electrons, where a nominal periodicity is conserved.

Additional evidence of the localized electron states was obtained by an examination of the temperature dependence of the capacitance of the Schottky devices fabricated with the SL's under investigation. In order to explain the experimental results, a simple two-miniband model with localized electron states in the lowest miniband, and with free electrons in the high-lying second one, has been developed. This model allows a qualitative explanation of the influences of the doping level and of the width of the miniband on the number of thermalized electrons contributing to the temperature dependence of the capacitance.

ACKNOWLEDGMENTS

The authors express their recognition to A. I. Toropov for sample preparation. Y.A.P. wishes to thank Professor R. Enderlein and Dr. S. S. Sokolov for helpful discussions. Financial support from CNPq, FAPESP, and CAPES is appreciated.

¹L. Esaki and R. Tsu, IBM J. Res. Dev. **14**, 61 (1970).

²C. Zener, Proc. R. Soc. London, Ser. A **145**, 523 (1934).

³L. Esaki, L. L. Chang, W. E. Howard, and V. L. Rideout, in *Proceedings of the 11th International Conference on the Physics of Semiconductors*, edited by the Polish Academy of Sciences (PWN-Polish Scientific Publishers, Warsaw, Poland, 1972), p. 431.

⁴R. Tsu and G. Döhler, Phys. Rev. B **12**, 680 (1975).

⁵J. Bleuse, G. Bastard, and P. Voisin, Phys. Rev. Lett. **60**, 220 (1988).

⁶A. Chomette, B. Deveaud, A. Regreny, and G. Bastard, Phys. Rev. Lett. **57**, 1464 (1986).

⁷Yu. A. Pusep, A. G. Milekhin, and A. I. Toropov, J. Phys. Condens. Matter. **6**, 93 (1994).

⁸Yu. A. Pusep, M. T. O. Silva, J. C. Galzerani, A. G. Milekhin, N. T. Moshegov, and A. I. Toropov, J. Appl. Phys. **79**, 8024 (1996).

⁹S.-R. E. Yang and S. Das Sarma, Phys. Rev. B **37**, 10 090 (1988).

¹⁰*Semiconductors, Physics of Group IV Elements and III-V Compounds*, edited by O. Madelung and H. Schulz, Landolt-Börnstein, New Series, Group III, Vol. 17, Pt. a (Springer-Verlag, Berlin, 1987).

¹¹D. Bimberg, D. Mars, J. N. Miller, R. Bauer, and D. Oertel, J. Vac. Sci. Technol. B **4**, 1014 (1986).

¹²D. Bimberg, J. Christen, T. Fukunaga, H. Nakashima, D. Mars, and J. N. Miller, J. Vac. Sci. Technol. B **5**, 1191 (1987).

¹³M. Li, *Modern Semiconductor Quantum Physics* (World Scientific, Singapore, 1994).